Journal of Alloys and Compounds 504 (2010) 514–518

Contents lists available at ScienceDirect

Journal of Alloys and Compounds

journal homepage: www.elsevier.com/locate/jallcom

The kinetics of Ni–Co/SiC composite coatings electrodeposition

B. Bahadormanesh [a], A. Dolati [b,*]

[a] Sharif University of Technology, Science and Engineering Department, Kish, Islamic Republic of Iran
[b] Sharif University of Technology, Materials Science and Engineering Department, Azadi Ave., Tehran, Islamic Republic of Iran

ARTICLE INFO

Article history:
Received 28 January 2010
Received in revised form 20 May 2010
Accepted 29 May 2010
Available online 11 June 2010

Keywords:
Ceramic
Coating materials
Metal matrix composites
Metal and alloys
Kinetics

ABSTRACT

Ni–Co/SiC composite coatings with various contents of SiC particles were electrodeposited in a modified Watt's type of Ni–Co bath containing suspended 20 nm SiC particles. Deposition parameters including current density, bath SiC concentration and magnetic stirring rate were optimized for the highest amount of the SiC codeposition: the current density of 4 A/dm^2, 40 g/dm^3 SiC concentration and 480 rpm stirring rate. In order to study the SiC particles codeposition, the Guglielmi's model of codeposition was modified for high volume percentages of the second phase and the modified model was employed to explain the effects of deposition parameters on the kinetics of the particles codeposition. Moreover, the influence of suspended SiC particles on the anomalous electrodeposition of Ni^{2+} and Co^{2+} ions was studied. In the presence of these particulates, anomalous electrodeposition of Ni^{2+} and Co^{2+} ions was enhanced.

1. Introduction

Quite a lot of reports have been published on metal matrix composite coatings fabricated through electro-codeposition of particles with metallic ions. The most employed matrices have been nickel and its alloys and the incorporated reinforcements usually had been carbides, silicides, nitrides, metal powders and oxides. These coatings are extensively studied with the object of hardness and wear resistance amelioration, improving of anti-corrosion properties, impartation of self-lubrication characteristics and obtaining higher service temperatures [1–8]. With the increasing availability of ever decreasing particle sizes, quite many scholars have investigated to greatest extent on incorporation of micron, submicron and nano-particles in metallic matrices. According to our previous work, a reduction in SiC particle size from micro- to nano-scale improves the mechanical performance of the Ni/SiC composite coatings such as hardness and scratch resistance [9]. The major challenge in the composite electrodeposition has been codeposition of high levels of non-agglomerated finely dispersed particles. Therefore, conduction of this relatively simple and cost effective method is affected by attempts of the researchers toward solving of this crucial problem. In addition to usage of different surfactants in deposition bath, electrodeposition under magnetic field and under ultrasound condition are some of the techniques employed for preventing of the particles from agglomeration [10,11].

Ni–Co alloys are usually known owing to their favorable properties such as good mechanical performance, resistance to wear and corrosive environments, thermal stability and magnetism [12–18]. These special characteristics of Ni–Co alloys have made them convenient for widespread applications as metallic matrix; and various particles have been incorporated in, through electrochemical methods, such as Cr_2O_3 [19], carbon nano-tube (CNT) [20], Yttria stabilized Zirconia Alumina (YZA) [21], SiC [22,23,24], Al_2O_3 [25,26] diamond [27], MoS_2 [28], $LaNi_5$ [29], barium ferrite [30], and Si_3N_4 [31].

Electrodeposition of Ni and Co ions is an anomalous type that the less noble metal (cobalt) deposits preferentially and the Co ratio Co/(Ni + Co) in the deposits is higher than that of the solution [14,16,18,21,32]. Nevertheless, reports on influences of suspended particles on the anomalous electrodeposition of Ni and Co are scarce. However, there are some evidences that the presence of these particles in the deposition electrolyte can increase the codeposition of Co and vice versa; the addition of Co to Ni deposition bath can increase the particles content of the coating [23,25,26].

During last decades, many researches were concentrated on the electro-codeposition of composite coatings with enhanced mechanical, corrosion and tribological properties. As a result, reports have been published on the deposition of composite coatings and their corresponding characteristics. Apart from massive achievements in this area, the codeposition mechanism of inert particles is not fundamentally understood. Guglielmi [33] was the first proposed a model describes quantitatively the current density and particle loading effects on the particles codeposition rate, based on a physical-electrochemical mechanism of adsorption. According to this model, the particles incorporation in metallic matrix

* Corresponding author. Tel.: +98 21 6022721; fax: +98 21 6005717.
E-mail addresses: Behrouz_Bahadormanesh@yahoo.com (B. Bahadormanesh), Dolati@Sharif.edu (A. Dolati).

0925-8388/$ – see front matter © 2010 Elsevier B.V. All rights reserved.
doi:10.1016/j.jallcom.2010.05.154

occurs in two sequential steps of adsorption. In the first step called loose adsorption, ion coated particles reversibly adsorb on the cathode surface and produce a high degree of coverage. This step of adsorption has physical characteristics. The strong adsorption of the particles occurs in the second step which is electrochemical in character. Reduction of ions adsorbed on the particles produces the circumstance of irreversible strong adsorption. Then, the particles progressively are engulfed by the growing metallic matrix. The mentioned model can be summarized by:

$$\frac{C(1-\alpha)}{\alpha} = \frac{Wi_0}{nFd\upsilon_0} e^{(A-B)\eta}\left(\frac{1}{K}+C\right) \quad (1)$$

and

$$\sigma = \frac{KC}{1+KC}(1-\theta) \quad (2)$$

where α is the volume fraction of the particles in the coating, C is the volume fraction of the particle in the bath, W is the atomic weight of the deposited metal, n is the valence of the deposited metal, F is the Faraday's constant, d is the density of the deposited metal, i_0 and A are the constants related to the metal deposition, υ_0 and B are the constants related to the particle deposition, K is the adsorption coefficient, η is the deposition overpotential, σ loose adsorption coverage and θ strong adsorption coverage. The validity of Guglielmi's model has been verified by various composite deposition baths [33–38]. Also, the model has been modified by Berçot et al. through considering hydrodynamic effects [34]. Some other models have been proposed, including the Celis and Trajectory models. In the Celis model, the primary hypothesis is that particles will be embedded only if a certain number of adsorbed ions on the particles surface is reduced (a statistical treatment of the particle incorporation) [39]. In the Trajectory model, the codeposition rate is determined via considering the fluid flow, taking into account all the forces acting on the particle and assuming that particles will incorporate in the matrix once the contact with the electrode surface occurs [40].

As mentioned, reports on the mechanism of composite coatings electrodeposition are scanty. Thus, the present work aims to investigate the codeposition mechanism of the SiC particulates with Ni^{2+} and Co^{2+} ions from an additive free Watt type bath. To this end, the Guglielmi's model of codeposition was modified for electrocodeposition of high volume percentage of the second phase and the modified model was employed to explain the effects of current density and particle loading and stirring rate of the bath on the kinetics of the particles codeposition. Moreover, the influence of suspended SiC particles on the anomalous electrodeposition of Ni^{2+} and Co^{2+} ions was studied.

2. Experimental

Modified electrolytes were based on Watt's bath for Ni–Co alloy deposition with different amounts of 20 nm SiC, their compositions are listed in Table 1. Analytical reagents and triple distilled water were used for the solutions preparation. In order to prevent agglomeration of the SiC particles, electrolytes containing the particles were premixed and stirred by a magnetic stirrer for 24 h and subsequently by ultrasonic agitation (power of 350 W and frequency of 40 kHz) for 30 min just prior to electrodeposition. 100 cc beaker was used as the deposition bath and the volume of the electrolytes were 100 cc. Three vertical electrodes set up was employed for the codeposition process. The electrochemical depositions were conducted by an IM6 model Zahner potentiostat/galvanostat controlled by Thales software. A nickel plate (99.9% purity) was used as anode with dimensions of 6 cm × 1 cm × 0.1 cm and up to 3 cm of its length was immersed in electrolyte. Cathodes were copper plate with a size of 1 cm × 2 cm × 0.1 cm, mechanically polished to 2000-grit finish with SiC papers and chemically pre-treated by immersing in acetone for 15 min. The cathode plates were inserted in a PTFE holder with a 7 mm circular window exposed to the electrolyte. Deposition current densities were 1–6 A/dm^2 and the coating thicknesses were 8 μm.

The percentage of SiC in the coatings was determined using energy dispersive X-ray spectroscope (EDS) system attached to scanning electron microscope (SEM, Rontec model). The deposits were stripped in 1:3 HNO_3 solution, and then the amounts of cobalt and nickel were measured using atomic absorption spectroscope (AAS, GBC model).

Table 1
Composition of the bath and deposition parameters.

$NiSO_4{\cdot}6H_2O$	220 g/dm^3
$NiCl_2{\cdot}6H_2O$	40 g/dm^3
$CoSO_4{\cdot}7H_2O$	20 g/dm^3
H_3BO_3	30 g/dm^3
20 nm SiC	0, 10, 20, 30, 40 g/dm^3
pH	4.2
Temperature	50 °C
Current density	1, 2, 3, 4, 5, 6 A/dm^2

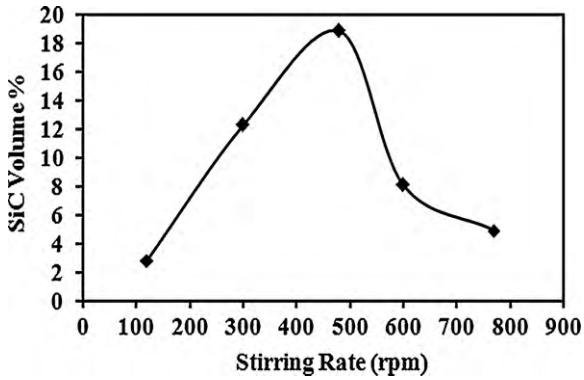

Fig. 1. Correlation between the volume percentage of SiC and stirring rate.

3. Results and discussion

3.1. Effects of stirring rate on the codeposition of the SiC particle

In order to optimize stirring rate, five stirring rates were selected between 120 and 770 rpm. The arbitrary current density of 2 A/dm^2 was applied for deposition. As it is observed in Fig. 1, the particles content of the coating with 480 rpm is higher than others. The rest of the experiments were conducted with 480 rpm stirring rate. An optimum stirring rate has been reported by other researchers for electrodeposition of many composite systems such as Ni–Co/Al_2O_3 and Ni–Co/SiC composite coatings [22,24,26]. Although Guglielmi's model does not consider directly hydrodynamic effects on the codeposition phenomenon, it seems that as the stirring rate increases initially, the capability of fluid flow for transporting of the particles to the cathode surface increases and consequently the loose adsorption coverage of the particles increases; however, when the stirring rate is higher than the optimum value, the loosely adsorbed particles are swept away from the cathode surface by the fluid flow and collision of non-adsorbed particles. Hence, the rate of the particles desorption is enhanced and lower percentages of the loosely adsorbed particles have the chance of transference from loose adsorption to strong adsorption step.

3.2. Effects of current density on the cobalt ratio in the deposits

Fig. 2 shows the relationship between current density and Co ratio in the alloy and composite coatings obtained by the AAS analyses. In both types of the coatings, the Co ratio exhibits a decreasing trend by increasing the current density. In these solutions, the Co ions concentration is low (about 0.07 mol/dm^3) in the deposition baths and so cobalt is under diffusion control. Whereas, nickel is controlled kinetically as its concentration is so high (about 1 mol/dm^3). Higher current densities provide more reductive circumstance and consequently more activation energy for deposition. This is more beneficial for deposition of the species controlled kinetically than that controlled by diffusion. Therefore,

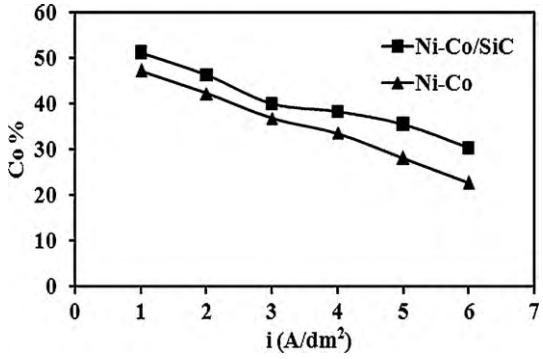

Fig. 2. Co% in Ni–Co alloy and Ni–Co/SiC composite coatings as a function of current density.

increasing the current density, the contribution of Ni ions in electron transfer is enhanced and its content in the deposits increases, which is equivalent to the reduction of the relative amount of cobalt in the deposits.

It is worth to note that in all the current densities and in both types of the coatings, the Co ratio in the deposits is higher than that of the deposition bath (the Co ratio in the deposition bath is approximately 1/13), which shows the anomalous behavior of the Ni and Co codeposition.

Another point should be paid attention is that in all the current densities, the Co content of the composite coating is higher than that of the alloy coating which demonstrates that the anomalous deposition of Ni and Co is enhanced in the presence of the SiC particles. Such a phenomenon has been pointed out by Wu et al. [25,26] for the codeposition of Al_2O_3 and by Srivastava et al. [23] for codeposition of SiC particles with Ni and Co ions. The difference in the absorbability of Ni and Co ions to the SiC particulates accounts for the enhancement of the Co^{2+} deposition. The absorbability of Co ions to SiC particulates is more than that of Ni^{2+} ions [23,25,26].

3.3. Kinetic of particle deposition

3.3.1. Particles content versus current density

The criterion for the selection of the optimum current density was the codeposition of highest volume percentage of the SiC particles. Current densities from 1 to 6 A/dm^2 were applied. Fig. 3 shows the correlation between the SiC volume percentage and current density. It is observed that the content of the codeposited SiC particles increases initially with the current density and reaches a maximum at the current density of 4 A/dm^2. As the current density surpasses this value, the volume percentage of the deposited SiC particulates decreases. Such a behavior has been observed in other reports [22,26]. Details of the current density effects on engulfing rate of the SiC particles will be discussed based on Guglielmi's model.

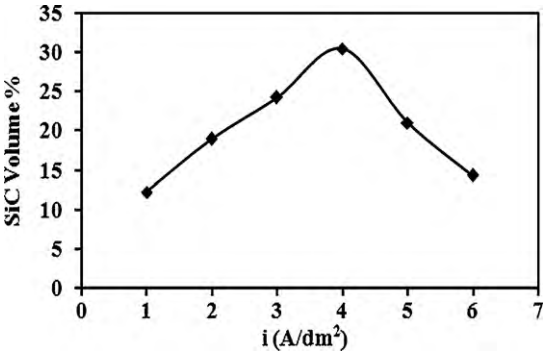

Fig. 3. Corellation between the SiC volume percentage and current density.

3.3.2. Adaptation of Guglielmi's model for the Ni–Co/SiC composite coatings

Being simple and effective, Guglielmi's model was employed to describe mathematically the influences of current density and bath particle loading on the incorporation rate of the SiC particles in the Ni–Co matrix.

As reviewed, the mentioned model can be summarized by Eqs. (1) and (2). In the cases of the low volume fractions of the second phase, $1-\alpha$ can be ignored in Eq. (1) and the original equation is estimated by the following:

$$\frac{C}{\alpha} = \frac{Wi_0}{nFd\upsilon_0} e^{(A-B)\eta}\left(\frac{1}{K}+C\right) \tag{3}$$

However, in our composite system relatively high volume fractions of the SiC were codeposited; thus, the Eq. (1) should be employed.

Assuming the particles are of regular shape, the strong adsorption coverage θ can be estimated by α [33]. Considering the reduction of effective cathode surface area for deposition by predeposited nonconductive particles and employing Butler–Volmer equation for high overpotentials $i = i_0 e^{A\eta}$, the following approximation is reasonable:

$$i = (1-\alpha) i_0 e^{A\eta} \tag{4}$$

So

$$i_0 e^{(A-B)\eta} = i_0 (e^{A\eta})^{(1-B/A)} = i_0^{B/A}\left(\frac{i}{1-\alpha}\right)^{(1-B/A)} \tag{5}$$

Substituting right hand side of Eq. (5) in Eq. (1), a generalized expression of Guglielmi's model can be obtained for nonconductive particles and without previous approximations due to low volume fractions of second phase:

$$\frac{C(1-\alpha)}{\alpha} = \frac{Wi_0^{B/A}}{nFd\upsilon_0}\left(\frac{i}{1-\alpha}\right)^{(1-B/A)}\left(\frac{1}{K}+C\right) \tag{6}$$

In this equation, due to the dependence of $i/(1-\alpha)$ to C there is no linear relationship between the left hand side of the equation and C. So, contrary to previous studies, to obtain K, we cannot plot the left hand side of the equation versus C, linearly. Rearranging the equation, we have:

$$\frac{C(1-\alpha)^{(2-B/A)}}{\alpha} = \frac{Wi_0^{B/A}}{nFd\upsilon_0} i^{(1-B/A)}\left(\frac{1}{K}+C\right) \tag{7}$$

Now, there is a linear relationship between $C(1-\alpha)^{(2-B/A)}/\alpha$ and C that the intercept on abscissa can be equated to $-1/K$, giving the adsorption constant K. However, B/A in the left side is unknown. To solve this problem, taking logarithm from Eq. (6) as following:

$$\log\left(\frac{C(1-\alpha)}{\alpha}\right) = \log\left(\frac{Wi_0^{B/A}}{nFd\upsilon_0}\right) + \left(1-\frac{B}{A}\right)\log\left(\frac{i}{1-\alpha}\right) + \log\left(\frac{1}{K}+C\right) \tag{8}$$

and plotting $\log(C(1-\alpha)/\alpha)$ against $\log(i/(1-\alpha))$, yields straight lines that their slops give hand the $1-B/A$ and B/A can be computed.

Fig. 4 presents the linear regression of $\log(C(1-\alpha)/\alpha)$ versus $\log(i/(1-\alpha))$ for the codeposition of the nano-sized SiC. It would be worth mentioning that since these lines are parallel, the ratio B/A remains constant regardless of the variations of the SiC concentration and current density. The calculated B/A ratio is 1.685. Constant B being greater than constant A, freely solvated metal ions are reduced slower than metal ions adsorbed on the particles

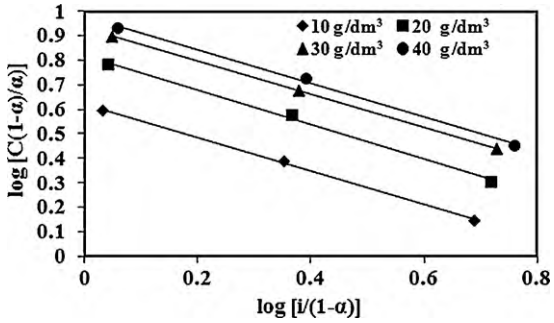

Fig. 4. Variation of the linear regression of $\log(C(1-\alpha)/\alpha)$ against $\log(i/(1-\alpha))$ for B/A ratio calculation.

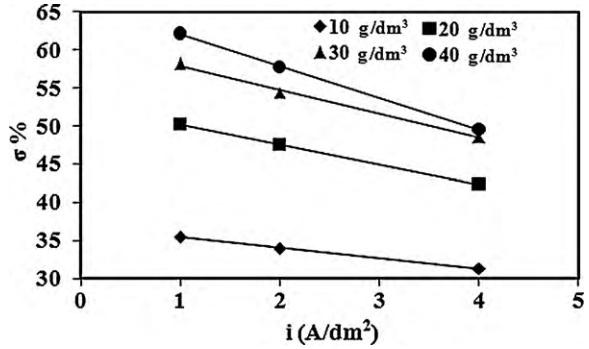

Fig. 6. Variation of the loose adsorption coverage in the different current densities.

surface and an increase in the current density leads to the higher volume fractions of the SiC particles in the deposits. Of course, as seen in Fig. 3, this increase in the volume percentage of the second phase continues up to the current density of 4 A/dm^2 and after that decreasing trend starts.

In order to estimate the adsorption constant K, calculated B/A was substituted in Eq. (7). Fig. 5 depicts the linear fitting lines of the $C(1-\alpha)^{(2-B/A)}/\alpha$ versus C for the different current densities. Adsorption coefficient K for the nano-particles is equal to 2. Either K and B/A ratio are in the same order of magnitude for the codeposition of 62 nm SiC particles with Ni from a sulfamate bath [36]. Substituting K values in Eq. (2), the surface concentration of the loosely absorbed particles can be determined. The loose and strong adsorption coverage of the SiC particles on the cathode surface is tabulated in Table 2 for the different current densities and various SiC concentrations.

It is seen in Table 2 that in all the current densities and SiC concentrations, the loose adsorption of the particles is much higher than their concentration in the electrolytes. In addition, in all the current densities and concentrations, the strong adsorption coverage of the particles is much lower than the loose adsorption of them and just a fraction of the loosely adsorbed particles can be codeposited through the reduction of the metallic ions surrounding them. This demonstrates that the strong adsorption of the particles is the rate determining step in the codeposition process.

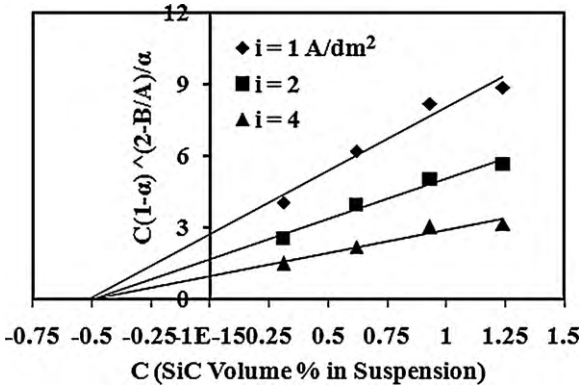

Fig. 5. Linear fitting lines of the $C(1-\alpha)^{(2-B/A)}/\alpha$ versus C for the different current densities.

Table 2
Loose and strong adsorption coverage in various current densities and bath concentrations.

SiC vol.%	Current density					
	1 A/dm^2		2 A/dm^2		4 A/dm^2	
	σ%	θ%	σ%	θ%	σ%	θ%
0.31	35.48	7.27	33.98	11.21	31.36	18.04
0.62	50.20	9.31	47.52	14.14	42.38	23.44
0.93	58.18	10.53	54.39	16.36	48.60	25.26
1.24	62.19	12.72	57.75	18.95	49.55	30.47

Fig. 6 shows the variation of the loose adsorption coverage of the nano-particles versus current density. The reduction trend of the loose adsorption coverage is obvious. The difference in the mechanism of ions and particles mobility accounts for this reduction. The motion of the ions and particles in the deposition bath is due to the agitation of the electrolyte and electrical field. The dominant cause of the particles motion toward the cathode surface is the agitation of the electrolyte. On the other hand, the role of electrical field in the ions mobility is more pronounced. The stirring rate of the electrolyte being constant, the increase in the current density has not much effect on the particles mobility, but enhances the mobility of the free ions and consequently lessens the particles relative concentration around the cathode. Moreover, because the deposition electrolyte is too concentrated (about 1 mol/dm^3), the overall metal deposition process is under kinetic control and increasing in current density, the ions flux to the cathode surface increases progressively. However, particles flux behaves differently by current density variations. According to Vereecken et al. [41], particles flux J_p depends on ν the kinematic viscosity of the solution (cm^2 s^{-1}), D_p the diffusion coefficient for the particles (cm^2 s^{-1}), $C_{p,b}$ the particle concentration in the bulk solution, $C_{p,s}$ the particle concentration at the surface and w the rotation rate of the electrode (S^{-1}):

$$J_p = -1.554\nu^{-1/6}D_p^{2/3}(C_{p,b} - C_{p,s})w^{1/2} \quad (9)$$

The surface concentration of the particles $C_{p,s}$ is dependent on the deposition current density. As the current density increases, $C_{p,s}$ decreases and approaches to zero and thereby J_p increases up to a constant maximum value. In other words, after a definite current density, J_p is controlled by diffusion of SiC particulates to the cathode surface. Therefore, as the current density surpasses the value corresponds to $C_{p,s} = 0$, an increase in the current density, increases the freely solvated ions flux but has no further effect on the particles flux. So, the particles relative concentration around the cathode reduces and the chance of the loose adsorption of them to the cathode surface decreases. Another plausible explanation for the reduction of the loose adsorption coverage can be the occurrence and enhancement of hydrogen evolution side reaction in higher current densities [42,43]. As the current density increases, hydrogen bobbles generation is enhanced. The bobbles, which their initial sizes are in the order of the particles not the ions, obstruct the particles approach track to the cathode surface more than that of the ions. Hence, the particles concentration around the cathode surface and their loose adsorption reduces. The outcome of these effects is the reduction in the loose adsorption coverage of the particles.

In spite of this reduction trend in the loose adsorption of the particles by increasing in the current density, the rate of the particles

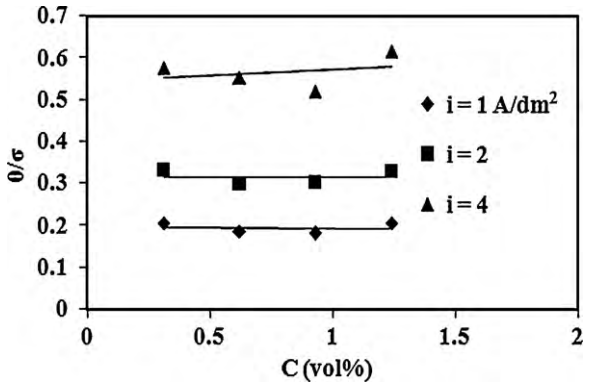

Fig. 7. Loose adsorption to stronge adsorption tranference efficiency in the various current densities.

incorporation increases (early parts of Fig. 2). This seems justified while considering the fact that according to Guglielmi's model, the strong adsorption of the particles controls the codeposition process. To clarify, θ/σ ratios are calculated and the results are summarized in Fig. 7. It is seen that the θ/σ ratio for a definite current density remains constant whatever the SiC concentration in the bath and it increases as the current density increases. It reveals that although the loose adsorption coverage has a reduction trend by increasing the current density, the transfer efficiency of the particles from the loose adsorption step to strong adsorption step increases, resulting in higher strongly adsorbed particles. In other words, the increase in the current density leads to two effects: the reduction of the loose adsorption coverage and higher probability of transfer from the loose adsorption step to strong adsorption step. It can be inferred that there is an optimum current density, which is the resultant of these two effects, corresponds to the highest particles incorporation. In current densities higher than the optimum one, although the probability of the particles transference from the loose adsorption step to strong adsorption step increases, there would not be enough loosely adsorbed particles for transference. Fig. 3 shows this optimum current density for the nano-SiC incorporation.

4. Conclusions

Ni–Co/SiC composite coatings were deposited from the modified Watt's type bath. The deposition parameters were optimized to obtain maximum particle codeposition: 40 g/dm^3 SiC and 480 rpm stirring rate and the current density of 4 A/dm^2. The presence of the nano-SiC particles enhanced the anomalous behavior of nickel and cobalt electrodeposition. The reverse dependence of cobalt percentage with current density was due to the fact that Co ions concentration was much lower than that of Ni ions and its deposition was under diffusion control. The Guglielmi's model of particle codeposition was modified for the deposition of high volume percentages of the second phase and previous approximations due to the low volume fraction of the second phase were removed. The general proposed equation was:

$$\frac{C(1-\alpha)^{(2-B/A)}}{\alpha} = \frac{Wi_0^{B/A}}{nFd\upsilon_0} i^{(1-B/A)} \left(\frac{1}{K} + C\right)$$

The increase in the current density during codeposition has two consequences: (a) the reduction of the loose adsorption coverage and (b) the higher probability of transfer from the loose adsorption step to the strong adsorption step. The existence of an optimum value for the codeposited SiC volume percentage by increasing the current density was attributed to the resultant of decreasing trend in the loose adsorption coverage and increasing trend in the transference probability from the loose adsorption step to the strong adsorption step.

References

[1] S.T. Aruna, V.K. William Grips, K.S. Rajam, J. Alloys Compd. 468 (2009) 546–552.
[2] Q. Li, X. Yang, L. Zhang, J. Wang, B. Chen, J. Alloys Compd. 482 (2009) 339–344.
[3] J. Panek, A. Budniok, Surf. Coat. Technol. 201 (2007) 6478–6483.
[4] L. Benea, F. Wenger, P. Ponthiaux, J.P. Celis, Wear 266 (2009) 398–405.
[5] A. Zoikis-Karathanasis, E.A. Pavlatou, N. Spyrellis, J. Alloys Compd. 494 (2010) 396–403.
[6] H. Ataee-Esfahani, M.R. Vaezi, L. Nikzad, B. Yazdani, S.K. Sadrnezhaad, J. Alloys Compd. 484 (2009) 540–544.
[7] A.A. Aal, H.A. Gobran, F. Muecklich, J. Alloys Compd. 473 (2009) 250–254.
[8] B.M. Praveen, T.V. Venkatesha, J. Alloys Compd. 482 (2009) 53–57.
[9] A. Sohrabi, A. Dolati, M. Ghorbani, A. Monfared, P. Stroeve, Mater. Chem. Phys. 121 (2010) 497–505.
[10] C. Wang, Y. Zhong, J. Wang, Z. Wang, W. Ren, Z. Lei, Z. Ren, J. Electroanal. Chem. 630 (2009) 42–48.
[11] F.F. Xia, C. Liu, F. Wang, M.H. Wu, J.D. Wang, H.L. Fu, J.X. Wang, J. Alloys Compd. 490 (2010) 431–435.
[12] A. Dolati, M. Sababi, E. Nouri, M. Ghorbani, Mater. Chem. Phys. 102 (2007) 118–124.
[13] G.D. Hibbard, K.T. Aust, U. Erb, Mater. Sci. Eng. A 433 (2006) 195–202.
[14] L. Wang, Y. Gao, Q. Xue, H. Liu, T. Xu, Appl. Surf. Sci. 242 (2005) 326–332.
[15] L.M. Chang, M.Z. An, S.Y. Shi, Mater. Chem. Phys. 94 (2005) 125–130.
[16] M. Srivastava, V.E. Selvi, V.K.W. Grips, K.S. Rajam, Surf. Coat. Technol. 201 (2006) 3051–3060.
[17] K.R. Marikkannu, G.P. Kalaignan, T. Vasudevan, J. Alloys Compd. 438 (2007) 332–336.
[18] A. Ghahremaninezhad, A. Dolati, J. Alloys Compd. 480 (2009) 275–278.
[19] K. Kumar, R. Chandramohana, D. Kalyanaraman, Appl. Surf. Sci. 227 (2004) 383–386.
[20] L. Shi, C.F. Sun, P. Gao, F. Zhou, W.M. Liu, Surf. Coat. Technol. 200 (2006) 4870–4875.
[21] M. Srivastava, V.K.W. Grips, K.S. Rajam, J. Appl. Electrochem. 88 (2008) 669–677.
[22] L. Shi, C. Sun, P. Gao, F. Zhou, W. Liu, Appl. Surf. Sci. 252 (2006) 3591–3599.
[23] M. Srivastava, V.K.W. Grips, A. Jain, K.S. Rajam, Surf. Coat. Technol. 202 (2007) 310–318.
[24] M. Srivastava, V.K.W. Grips, K.S. Rajam, Appl. Surf. Sci. 253 (2007) 3814–3824.
[25] G. Wu, N. Li, D.L. Wang, D.R. Zhou, B.Q. Xu, K. Mitsuo, Mater. Chem. Phys. 87 (2004) 411–419.
[26] G. Wu, N. Lia, D. Zhou, K. Mitsuo, Surf. Coat. Technol. 176 (2004) 157–164.
[27] M. Pushpavanam, H. Manikandan, K. Ramanathan, Surf. Coat. Technol. 201 (2007) 6372–6379.
[28] L. Shi, C. Sun, W. Liu, Appl. Surf. Sci. 254 (2008) 6880–6885.
[29] G. Wu, N. Li, C.S. Dai, D.R. Zhou, Mater. Chem. Phys. 83 (2004) 307–314.
[30] S. Pané, E. Gómez, E. Vallés, J. Electroanal. Chem. 615 (2008) 117–123.
[31] M. Srivastava, V.K.W. Grips, K.S. Rajam, J. Alloys Compd. 469 (2009) 362–365.
[32] L.D. Rafailovic, H.P. Karnthaler, T. Trisovic, D.M. Minic, Mater. Chem. Phys. 120 (2010) 409–416.
[33] N. Guglielmi, J. Electrochem. Soc. 119 (1972) 1009–1012.
[34] P. Berçot, E. Pena-Munoz, J. Pagetti, Surf. Coat. Technol. 157 (2002) 282–289.
[35] R. Narayan, B.H. Narayana, J. Electrochem. Soc. 128 (1981) 1704–1708.
[36] S. Wang, W.J. Wei, Mater. Chem. Phys. 78 (2003) 574–580.
[37] Y.C. Chang, Y.-Y. Chang, C.-I. Lin, Electrochim. Acta 43 (1998) 315–324.
[38] H. Liu, W. Chen, Surf. Coat. Technol. 191 (2005) 341–350.
[39] J.P. Celis, R. Roos, C. Buelens, J. Electrochem. Soc. 134 (1987) 1402–1407.
[40] J. Fransaer, J.P. Celis, J.R. Roos, J. Electrochem. Soc. 130 (1992) 413–425.
[41] P.M. Vereecken, I. Shao, P.C. Searson, J. Electrochem. Soc. 147 (2000) 2572–2575.
[42] W.E.G. Hansal, B. Tury, M. Halmdienst, M.L. Varśanyi, W. Kautek, Electrochim. Acta 52 (2006) 1145–1151.
[43] C.T.J. Low, R.G.A. Wills, F.C. Walsh, Surf. Coat. Technol. 201 (2006) 371–383.